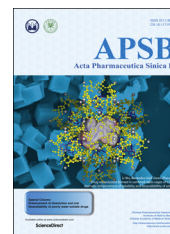




Chinese Pharmaceutical Association
Institute of Materia Medica, Chinese Academy of Medical Sciences

Acta Pharmaceutica Sinica B

www.elsevier.com/locate/apsb
www.sciencedirect.com



ORIGINAL ARTICLE

Selenium-layered nanoparticles serving for oral delivery of phytomedicines with hypoglycemic activity to synergistically potentiate the antidiabetic effect[☆]



Wenji Deng, Huan Wang, Baojian Wu*, Xingwang Zhang*

Department of Pharmaceutics, College of Pharmacy, Jinan University, Guangzhou 510632, China

Received 10 July 2018; received in revised form 10 August 2018; accepted 22 August 2018

KEY WORDS

Diabetes mellitus;
Phytomedicine;
Bioavailability;
Hypoglycemic effect;
Selenium nanoparticles

Abstract Diabetes mellitus (DM) remains a great challenge in treatment due to pathological complexity. It has been proven that phytomedicines and natural medicines have prominent antidiabetic effects. This work aimed to develop selenium-layered nanoparticles (SeNPs) for oral delivery of mulberry leaf and *Pueraria Lobata* extracts (MPE), a group of phytomedicines with significant hypoglycemic activities, to achieve a synergic antidiabetic effect. MPE-loaded SeNPs (MPE-SeNPs) were prepared through a solvent diffusion/*in situ* reduction technique and characterized by particle size, ζ potential, morphology, entrapment efficiency (EE) and drug loading (DL). The resulting MPE-SeNPs were 120 nm around in particle size with EE of 89.38% for rutin and 90.59% for puerarin, two marker components in MPE. MPE-SeNPs exhibited a slow drug release and good physiological stability in the simulated digestive fluid. After oral administration, MPE-SeNPs produced significant hypoglycemic effects both in the normal and diabetic rats. *Ex vivo* intestinal imaging and cellular examinations demonstrated that MPE-SeNPs were provided with outstanding intestinal permeability and transepithelial transport aptness. It was also revealed that MPE-SeNPs could alleviate the oxidative stress, improve the pancreatic function, and promote the glucose utilization by adipocytes. Our study provides new insight into the use of integrative nanomedicine containing phytomedicines and selenium for DM treatment.

© 2019 Chinese Pharmaceutical Association and Institute of Materia Medica, Chinese Academy of Medical Sciences. Production and hosting by Elsevier B.V. This is an open access article under the CC BY-NC-ND license (<http://creativecommons.org/licenses/by-nc-nd/4.0/>).

*Corresponding authors.

E-mail addresses: bj.wu@hotmail.com (Baojian Wu), zhangxw@jnu.edu.cn (Xingwang Zhang).

[☆]Invited for Special Column.

Peer review under responsibility of Institute of Materia Medica, Chinese Academy of Medical Sciences and Chinese Pharmaceutical Association.

<https://doi.org/10.1016/j.apsb.2018.09.009>

2211-3835 © 2019 Chinese Pharmaceutical Association and Institute of Materia Medica, Chinese Academy of Medical Sciences. Production and hosting by Elsevier B.V. This is an open access article under the CC BY-NC-ND license (<http://creativecommons.org/licenses/by-nc-nd/4.0/>).

1. Introduction

Diabetes mellitus (DM) has reached the epidemic dimension around the world. The rising incidence of DM brings a heavy burden to the society and individual family¹. A great number of oral hypoglycemic agents, such as biguanides and sulfonylureas, are available for DM treatment, but these synthetic hypoglycemic agents are connected to certain shortfalls², including hypoglycemia, gastrointestinal discomfort, liver impairment, and pancreatic degeneration. Phytomedicines applied for DM treatment have a long history. The traditional Chinese medicine (TCM) amassed a precious and wealthy experience in the treatment of DM, mastering plenty of phytomedicines and empirical prescriptions. Although phytomedicines and their active ingredients possess lower toxicity and side effects^{3,4}, it is still imperative to formulate them into more suitable dosage forms so as to potentiate their efficacy.

Nanomedicines are steering the development of medical/pharmaceutical sciences to a more precise dimension, specifically referring to various nano-formulations and drug delivery systems^{5–8}. Nanotechnology can substantially improve the *in vivo* delivery indices of therapeutic agents by the nanoscale effect. A variety of nano-drug delivery systems have been explored to orally deliver hypoglycemic agents, such as liposomes^{9–11}, micelles^{12,13}, nanoemulsions¹⁴, lipid nanoparticles^{15,16}, and sorts of polymeric nanoparticles^{17–20}. Hypoglycemic agents delivered *via* the oral route include both recombinant insulin²¹, and botanical ingredients against DM²². Some monomeric compounds from phytomedicines have also been investigated for their hypoglycemic activity, such as berberine²³, ginsenoside Rg1²⁴, and puerarin²⁵. These natural hypoglycemic agents demonstrate significant anti-diabetic effects, particularly in the case of berberine. Berberine formulated into nanoparticles not only enhanced the oral bioavailability, but also resulted in an explicit reduction of blood glucose^{26,27}. However, the pharmacological action of a single compound is relatively limited, especially in improving the pancreatic function. Herbal extracts contain a myriad of components that can remedy the metabolic disturbance of body through multiple pathways and multiple targets, which should be more effective in DM care.

Mulberry leaf and *Pueraria Lobata* are traditional phytomedicines used for DM care in the eastern countries. They have the potentials to inhibit α -glucosidase, stimulate insulin excretion, modulate the intestinal microflora, enhance the glucose utilization in the peripheral tissue, and activate the islet β cells^{28–31}. Although the exact pathogenesis of DM is not entirely clear, correlational studies show that some trace elemental nutrients are associated with DM. Selenium (Se) as a hypoglycemic cofactor has remarkable antioxidant and curative effects against DM^{32,33}. In addition, Se nanoparticles has been confirmed able to produce the hypoglycemic effect analogous to that of insulin³⁴. To date, there is no a therapeutic system containing Se and mulberry leaf and *Pueraria Lobata* extracts (MPE) available for DM.

In this study, we developed Se-layered nanoparticles (SeNPs) for oral delivery of MPE in an attempt to potentiate their antidiabetic effect. MPE-loaded SeNPs (MPE-SeNPs) were prepared by a solvent diffusion/*in situ* reduction technique and characterized by drug entrapment, particle size, morphology, *in vitro* release, and metabolic stability. The oral hypoglycemic

effect and bioavailability were investigated in normal and diabetic rats. The mechanisms of oral absorption and antidiabetic action on MPE-SeNPs were elucidated.

2. Materials and methods

2.1. Materials

Mulberry leaf and *Pueraria Lobata* were purchased from Tongrentang drugstore. Reduced L-glutathione, Na₂SeO₃ and Poloxamer188 were from Aladdin Reagent (Shanghai, China). PLGA_{10,000}-PEG₂₀₀₀ (50/50) and 1,2-dioleoyl-3-trimethylammonium-propane (DOTAP) were provided by RESENBio (Xi'an, China). Rutin and puerarin were purchased from Ruifensi Bio-Tech (Chengdu, China). Simvastatin, chlorpromazine, filipin, latrunculin B and ethylisopropylamiloride (EIPA) were purchased from Sigma-Aldrich (MO, USA). 1,1'-diocetadecyl-3,3',3'-tetramethylindocarbocyanine perchlorate (DiI) was obtained from Beyotime (Shanghai, China). HPLC-grade acetonitrile was provided by Merck Corp. (Darmstadt, Germany). All other chemicals were of analytical grade and used as received.

2.2. Preparation of MPE-SeNPs

First of all, the active constituents of mulberry leaf and *Pueraria Lobata* were respectively extracted using 75% ethanol (*v/v*) in a reflux tank with a crude material/solvent ratio of 1:10, concentrated in a rotary evaporator and lyophilized for use³⁵. MPE-SeNPs were prepared by the solvent diffusion/*in situ* reduction technique³⁶. Briefly, the botanical extracts comprising an aliquot of mulberry leaf extracts and two aliquots of *Pueraria Lobata* extracts (M/P = 1:2), PLGA-PEG, DOTAP and Poloxamer188 were dissolved in an aliquot of 75% alcohol and then quickly injected into 5 aliquots of water under stirring (1000 rpm, RH Basic 2, IKA, Staufen, Germany). Formulation components self-assembled into nanoparticles upon the solvent diffusion into the water. The resulting dispersions were subjected to homogenization with a high-pressure homogenizer to obtain the fine MPE-loaded nanoparticles (MPE-NPs). Then, Na₂SeO₃ was introduced into the system and stirred for 30 min at room temperature. After that, GSH was added into the nanosuspensions with a molar ratio of GSH to Na₂SeO₃ of 4:1. The reaction system was maintained at 37 °C and stirred at 1000 rpm (RH Basic 2, IKA, Staufen, Germany) for 2 h. MPE-SeNPs formed *in situ* when Se⁴⁺ was reduced to Se that precipitated onto the surface of MPE-NPs. The residual reactants were removed by dialysis against deionized water for three times. To obtain a preferred formulation, we studied the main factors affecting the formulation properties of MPE-SeNPs, including the percentage of poloxamer 188 used, the ratio of drug/excipients, the volume ratio of organic to aqueous phase upon preparation, and Na₂SeO₃ level used in the system.

2.3. Characterization of nanoparticles

Nanoparticles were characterized with particle size (PS), ζ potential, morphology, entrapment efficiency (EE) and drug loading (DL). PS and ζ potential were measured by Zetasizer Nano ZS (Malvern, UK) at 25 °C. Morphology of nanoparticles was observed by transmission electron microscopy (TEM, JEM-1230, JEOL, Japan). The micrographs were taken at an

acceleration voltage of 100 kV. EE and DL were determined after separating free drug from MPE-SeNPs through a centrifugal ultrafiltration technique³⁷. Untrapped components were firstly removed from the system by centrifugation at 5000 rpm (Centrifuge 5424R, Eppendorf, NY, USA), and then the purified MPE-SeNPs were subjected to centrifugal ultrafiltration using an MWCO 50 K filter device (Amicon[®], Millipore, USA). Free drug in the filtrate was quantified by HPLC as described below. EE and DL were calculated according to Eq. (1) and Eq. (2):

$$EE (\%) = \left(1 - \frac{M_{out}}{M_{tot}} \right) \times 100 \quad (1)$$

$$DL (\%) = \frac{M_{tot} - M_{out}}{(M_{tot} + M_{exc})} \times 100 \quad (2)$$

where M_{out} , M_{tot} and M_{exc} denote the amounts of free plus the untrapped drug, total drug and excipients used in the formulation, respectively. The drug for quantification is puerarin, a principal component in MPE.

2.4. *In vitro* release study

The reverse bulk equilibrium dialysis technique was utilized to study the release of rutin and puerarin, two marker compounds in MPE, from MPE-NPs and MPE-SeNPs. The release media included a pH 1.2 HCl solution, a pH 4.0 citrate buffer solution and pH 6.8 phosphate buffer solution. Briefly, several end-ligated dialysis bags containing 0.5 mL of blank medium were put into 250 mL of release medium in a dissolution cup. Then, 2 mL of MPE-NPs or MPE-SeNPs were added and reversely dialyzed against the dialysis membrane at 37 °C under magnetic stirring. At predetermined intervals, the dialysis bag was withdrawn, in which the concentrations of rutin and puerarin were determined by HPLC. Dionex UltiMate 3000 HPLC system equipped with a multichannel rapid scanning UV-Vis detector was used to quantify the marker components of MPE. The samples were eluted against a ZORBAX RX-C8 column (250 mm × 4.6 mm, 5 μm) at 30 °C and detected at 358 nm for rutin and 250 nm for puerarin. The mobile phase for rutin elution consisted of 45% methanol and 55% phosphoric acid solution (0.5%), and the mobile phase for puerarin elution comprised 35% methanol and 65% water pumped at a flow rate of 1.0 mL/min.

2.5. *Physiological stability of MPE in nanoparticles*

The ability of nanoparticles in protecting active components from enzymatic degradation was evaluated in the simulated intestinal fluid (SIF) containing the rat intestinal microsomes. Preparation of SIF and intestinal microsomes referred to reported procedures^{38,39}. MPE-NPs or MPE-SeNPs (1 mL) were added into 4 mL of digestive medium and incubated at 37 °C under shaking at 100 rpm (AS-MOR-3001, AS ONE, Shanghai, China). At predetermined time points, 200 μL of samples were withdrawn and neutralized with 200 μL of 0.1 mol/L HCl to terminate the degradation. Subsequently, the samples were treated with 100 μL of methanol and centrifuged at 12,000 × *g* and 4 °C for 10 min. Rutin and puerarin in the supernatants were quantified by HPLC. The percentages of retained rutin and puerarin were calculated by comparison with the initial values.

2.6. *Hypoglycemic effect and pharmacokinetics*

The hypoglycemic effects of MPE-SeNPs were studied in both Sprague-Dawley (SD) rats and Goto-Kakizaki (GK) rats. SD and GK rats (200 ± 20 g) were randomized into several groups (*n* = 6). The rats were fasted for 12 h before administration but freely accessible to water. Animals were maintained and treated according to the Guidelines on the Care and Use of Animals for Scientific Purposes (2004, Singapore), and the protocols for animal experiments were reviewed and approved by the Experimental Animal Ethical Committee of Jinan University (Guangzhou, China). The normal rats (SD) were orally given with saline, MPE solution (dissolved in 50% ethanol), MPE-NPs or MPE-SeNPs with an MPE dose of 125 mg/kg. In respect to MPE-SeNPs, they were composed of different M/P ratios (3:1, 2:1, 1:1, 1:2 and 1:3, respectively). The diabetic rats (GK) were orally administered with saline, MPE solution, SeNPs, MPE-NPs and MPE-SeNPs with a fixed M/P ratio or subcutaneously injected with insulin solution (1 IU/kg). After administration, an appropriate amount of blood (~250 μL) was sampled from the tail vein at predetermined intervals and immediately centrifuged at 5000 × *g* for 5 min to collect the plasma. The plasma glucose concentration was measured using a glucose assay kit (Jiancheng Bioengineering Institute, Nanjing, China). Meanwhile, rutin and puerarin concentrations in the plasma were determined by HPLC as established above. The pharmacokinetic parameters were processed with PKSolver 2.0, a freely available plug-in Excel program.

2.7. *Ex vivo* imaging of transepithelial transport

DiI-labeled MPE-NPs and MPE-SeNPs were utilized to investigate the intestinal epithelial permeability of nanocarriers by fluorescent imaging made to the intestinal tissue slices. Preparation of fluorescently labeled MPE-NPs and MPE-SeNPs followed the same procedure described above by incorporating DiI⁴⁰. SD rats were orally given DiI-labeled MPE-NPs and MPE-SeNPs with a dose of 125 mg/kg. The rats were killed by cervical dislocation 2 h after oral administration. Then, the entire small intestine of rats was excised and a 0.5-cm length of duodenum, jejunum and ileum was isolated, respectively. Subsequently, the intestinal segments were flushed with 4 °C saline for several times. After fixation with 4% paraformaldehyde, the intestinal segments were prepared into paraffin slices and stained with DAPI. Distribution of MPE-NPs and MPE-SeNPs in the absorptive epithelia was inspected by confocal laser scanning microscopy (CLSM, Zeiss LSM510, Oberkochen, Germany).

2.8. *Cellular uptake and trafficking pathway*

The cellular uptake of MPE-NPs and MPE-SeNPs was qualitatively evaluated on Caco-2 cells by CLSM imaging. DiI-labeled MPE-NPs and MPE-SeNPs were used to investigate the cellular internalization. MPE-NPs and MPE-SeNPs were incubated with Caco-2 cells for 0.25 h at 37 °C. After that, the cells were rinsed carefully and fixed with 4% paraformaldehyde. For comparative observation, the cell nuclei were further dyed with DAPI and then visualized by CLSM.

To clarify the cellular trafficking pathway of MPE-NPs and MPE-SeNPs, we probed into the uptake evolution of two kinds of nanocarriers on Caco-2 cells in the presence of transport inhibitors.

Caco-2 cells were pre-incubated with various physiological inhibitors at 37 °C for 0.5 h, then MPE-NPs and MPE-SeNPs were added into the cells and continued to incubate for another 2 h. Subsequently, the cells were washed carefully with Hank's balanced salt solution (HBSS). Intracellular drug (rutin) was analyzed by HPLC after extraction with 50% methanol by cell homogenization. The trafficking pathways of MPE-NPs and MPE-SeNPs were interpreted according to the relative cellular uptake under the action of transport inhibitors.

2.9. Hematological examination on oxidative stress

The oxidative stress level was measured in diabetic rats before and after treatment with MPE-NPs or MPE-SeNPs. GK rats were treated with MPE-NPs or MPE-SeNPs for two weeks at the daily dose of 125 mg/kg. After two weeks, an appropriate amount of blood was collected *via* the tail vein. The contents or activity of reactive oxygen species (ROS), malondialdehyde (MDA), superoxide dismutase (SOD), glutathione (GSH) and glutathione peroxidase (GSH-Px) were determined were measured with the relevant assay kits following the instructions of manufacturer (Jiancheng Bioengineering Institute, Nanjing, China).

2.10. Effects of MPE-SeNPs on pancreatic islet function and glucose utilization

The pancreatic islet function of GK rats was scored by immunofluorescence assay before and after treatment with MPE-NPs or MPE-SeNPs. The diabetic rats were orally given MPE-NPs or MPE-SeNPs (125 mg/kg) daily for two weeks. Afterwards, they were put to death, and their pancreases were excised and flushed. The pancreatic tissues were then fixed with 4% paraformaldehyde and prepared into paraffin sections. Pancreatic tissue sections from GK rats were then labeled with Cy3-conjugated antibody to insulin (ServiceBio, Wuhan, China) and DAPI. The viability of insulin secretion-associated cells was examined by the fluorescence intensity.

To investigate the effects of MPE-NPs and MPE-SeNPs on the glucose utilization in the peripheral tissue, adipocytes were constructed from adipose-derived stem cells (ADSCs) by induction of 3-isobutyl-1-methylxanthine (IBMX) (Supporting Information). Adipocytes were seeded in 48-well plates and cultured in 0.2% BSA culture medium for 48 h at 37 °C. MPE-NPs or MPE-SeNPs were then added into the wells, in which 25 mmol/L of glucose was simultaneously added. The cells treated with blank culture medium and insulin served as negative and positive control, respectively. At 2 and 4 h, the extracellular media were collected and the remaining glucose in which was determined using glucose assay kit. The glucose utilization was evaluated by the percentage of consumed glucose.

3. Results and discussion

3.1. Preparation and characterization of MPE-SeNPs

In general, a 75% ethanol solution exhibits the optimal permeability to both hydrophilic and hydrophobic substances. We utilized 75% ethanol to extract mulberry leaf and *Pueraria*

Lobata that guaranteed adequate extraction of active constituents with opposite solubility. Formulation variables that affect the PS and EE of MPE-NPs are shown in Fig. 1. The formulation with a high percentage of Poloxamer 188 could result in larger size of MPE-NPs, but higher EE (Fig. 1A). This suggests that the use of Poloxamer 188 is favorable for entrapment of MPE, rather than reduction of PS, since PLGA-PEG itself possesses an amphiphilicity that can self-assemble into nanoparticles. The role of Poloxamer 188 mainly facilitates MPE to be solubilized in PLGA, which accordingly will increase the thickness of the hydrophilic outer shell of nanoparticles. The MPE/excipients ratio has a great effect on the formulation properties of MPE-NPs (Fig. 1B). In this case, MPE-NPs with the smallest PS and highest EE were obtained at the MPE/excipients ratio of 1:4. It indicates that the loading capacity of PLGA-PEG for MPE is limited, and more MPE are not conducive to the formation of nanoparticles and encapsulation of drug. Another factor affecting the PS and EE of MPE-NPs was the volume ratio of organic phase to aqueous phase upon preparation (Fig. 1C). The phase ratio posed peculiar effects on PS and EE of MPE-NPs. MPE-NPs prepared with a phase ratio of 1:5 exhibited the smallest PS and highest EE. This may be associated with the optimal self-assembly space, requiring to be compact but not oppressive. MPE-SeNPs are fabricated on the basis of MPE-NPs by *in situ* reduction of Na₂SeO₃ with GSH. DOTAP acts as a cationic lipid to capture the selenite anion so as to Se attachment⁴¹. The Na₂SeO₃ concentration for reaction had a significant effect on the PS of MPE-SeNPs (Fig. 1D). The PS of MPE-SeNPs markedly went up with the increase of Na₂SeO₃ concentration. The PS has been over 200 nm as the Na₂SeO₃ comes to 0.12 mol/L. The sharp increase in PS can be attributed to considerable Se attachment to the surface of nanoparticles⁴².

Taking above together, we established the final formulation that consisted of 60 mg of MPE, 195 mg of PLGA, 30 mg of DOTAP and 15 mg of poloxamer 188 for MPE-NPs preparation, and 0.06 mmol of Na₂SeO₃ and 0.24 mmol of GSH for MPE-SeNPs preparation. Upon preparation, 2 mL of 75% alcohol were used and 10 mL of preparative volume were confirmed at last. The resulting MPE-NPs and MPE-SeNPs exhibited different appearances from pale yellow to red (Fig. 2A). They possessed a PS of 86 nm and 120 nm respectively, taking on a narrow distribution (Fig. 2B). The PS of MPE-SeNPs larger than MPE-NPs indicates the success of Se coating. It can be explained by nascent Se precipitation that increases the dimension of nanoparticles. Both MPE-NPs and MPE-SeNPs were spherical in morphology as revealed by TEM (Fig. 2C). The TEM micrograph of MPE-SeNPs turn up an apparent electron-dense layer around the nanoparticles, showing occurrence of Se layering. The EE of MPE-SeNPs for rutin and puerarin were determined to be as high as 90% with a drug loading of 5.25% and 10.64%, respectively. The absolute ζ potential of MPE-SeNPs was greater than 28 mV, implying an acceptable stability as colloidal dispersion system. The Se concentration in the MPE-SeNPs was approximately 0.466 mg/mL as quantified by ICP-AES³⁶. The dose of selenium administered to rats is approximately 900 μ g/day, which accounts to 150 μ g/day for human being according to dose conversion from rat to human. The daily intake level of selenium is far lower than the proposed dose (400 μ g/day) raised by World Health Organization (WHO, USA).

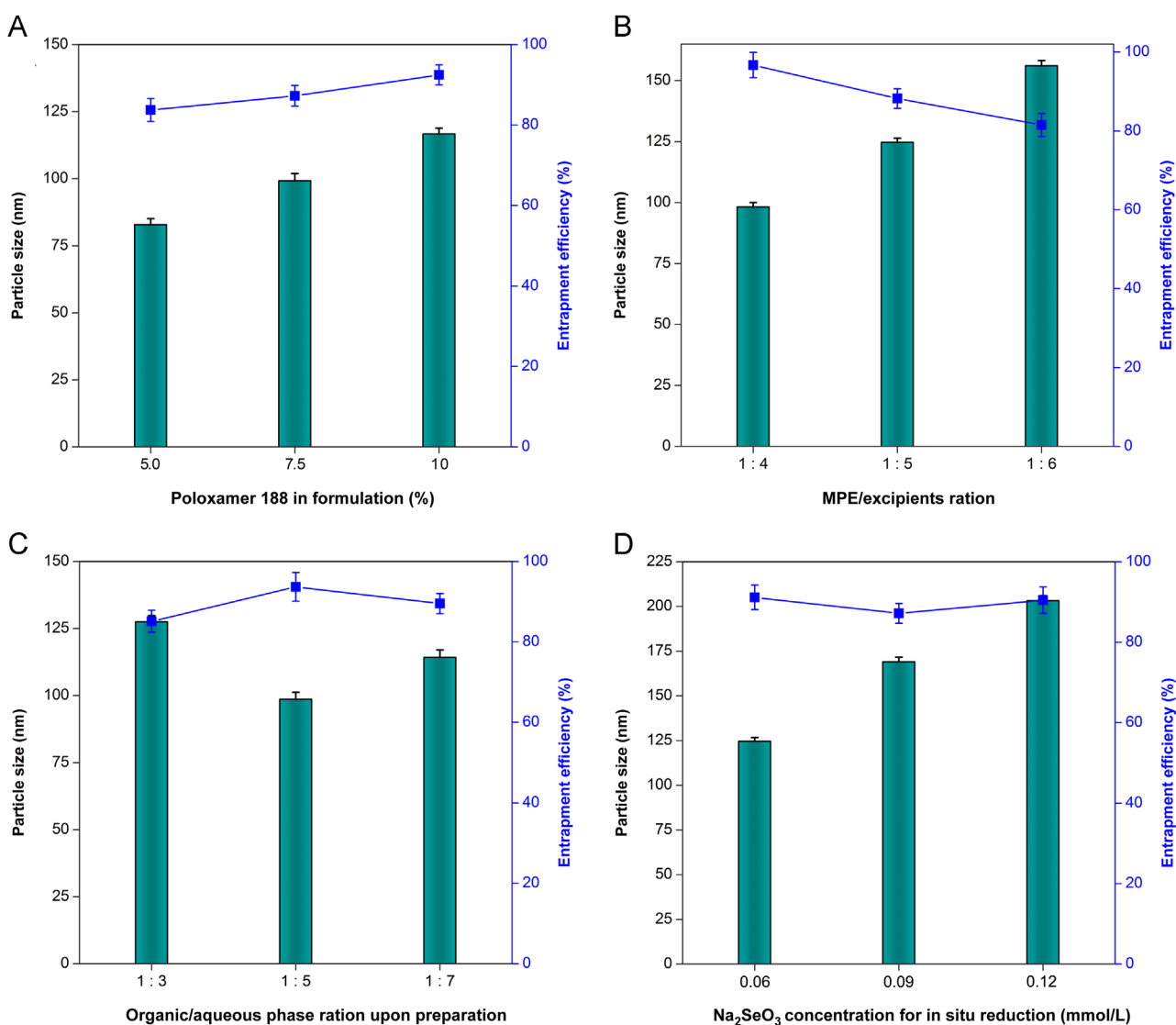


Figure 1 Effects of formulation variables on particle size and entrapment efficiency of MPE-SeNPs: Poloxamer percentage in formulation (A), MPE/excipients ratio (B), organic/aqueous phase ratio upon preparation (C) and Na₂SeO₃ concentration for *in situ* reduction (D).

3.2. Drug release from nanoparticles

The release profiles of rutin and puerarin from MPE-NPs and MPE-SeNPs in different media are shown in Fig. 3. In three kinds of media, MPE-NPs exhibited quicker drug release than MPE-SeNPs. The accumulative release percentages of rutin and puerarin exceeded 40% within 2 h in the case of MPE-NPs, whereas they were less than 30% in terms of MPE-SeNPs. At 24 h, approximately 80% active components are released from MPE-NPs, but only 60% from MPE-SeNPs. The phenomenon of quicker components release from MPE-NPs than MPE-SeNPs indicates that Se layering or coating can achieve a sustained drug release, which is favorable to circumvent the intestinal first-pass effect. In addition, a slow drug release can prolong the hypoglycemic effect of MPE-SeNPs *in vivo*⁴³. It is noteworthy that the coating layer of selenium is not completely leaktight as seen from Fig. 2C. The naked surface allows drug release from SeNPs through a diffusion mechanism.

3.3. Improved physiological stability through Se coating

One great challenge of oral drug delivery is the first-pass effect, including metabolisms both occurring in the intestine and in the liver. It is crucial to protect active ingredients from the intestinal degradation for oral drug delivery, especially for phytomedicine with multiple components. Fig. 4 shows the degradation profiles of marker components in MPE-NPs and MPE-SeNPs in the SIF containing intestinal microsomes. The marker components of rutin and puerarin in MPE-SeNPs exhibited a step-down degradation compared with those in MPE-NPs. SeNPs demonstrated a stronger stabilizing effect on MPE than non-selenylated nanoparticles. This may have relation to the structure reinforcement of nanoparticles due to selenium coating, but cannot exclude the factor of slow drug release. It has been reported that improving the intestinal stability of payloads can significantly enhance their oral bioavailability^{44,45}. Active components exerting the pharmacological effect greatly depend on their stability and amounts entering the systemic circulation. The stability test indicates that SeNPs can increase the

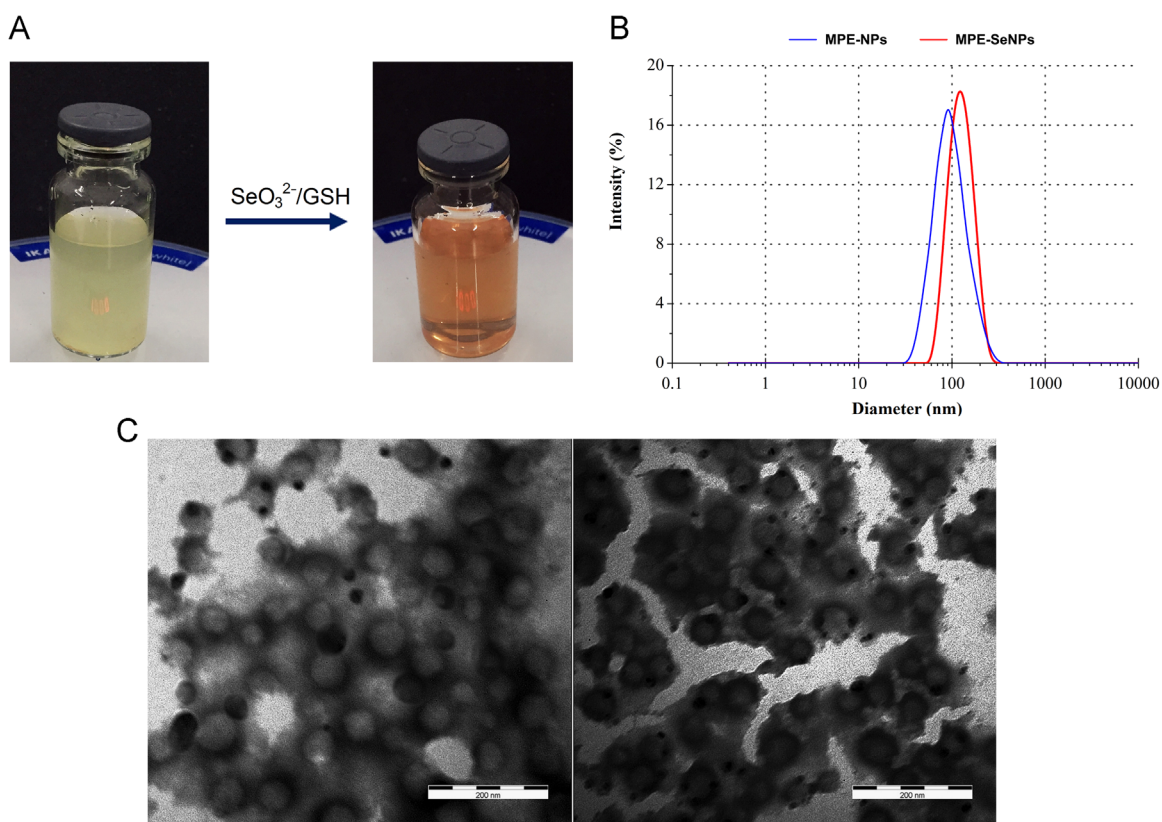


Figure 2 Preparation illustration and characterization of MPE-NPs and MPE-SeNPs: appearance (A), particle size distribution (B) and TEM micrographs (C). Scale: 200 nm.

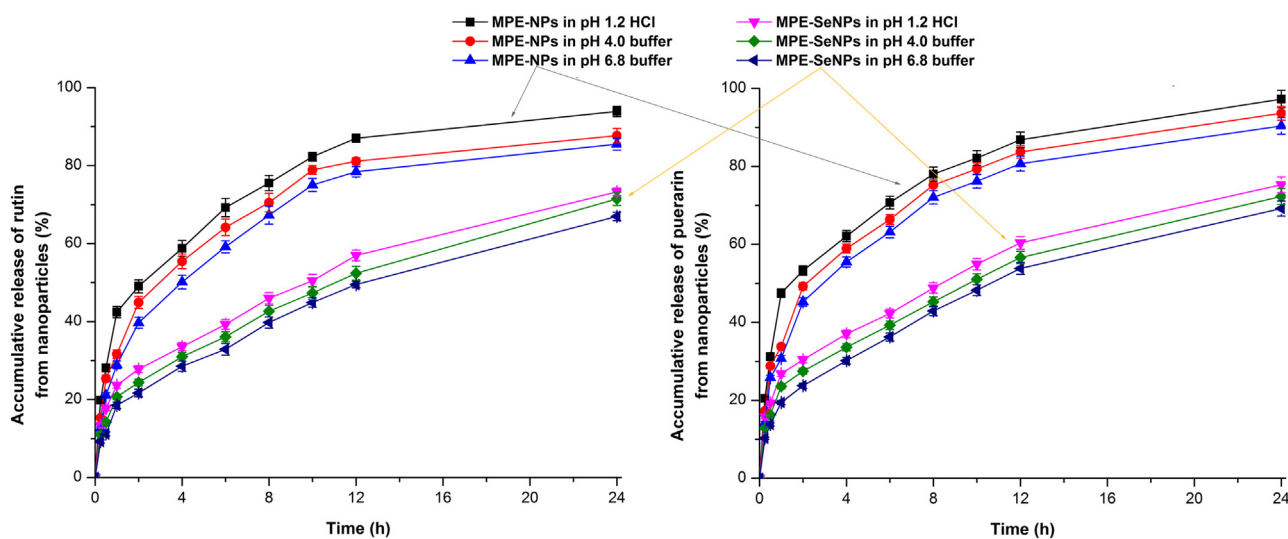


Figure 3 Release profiles of rutin and puerarin from MPE-SeNPs in pH 1.2 HCl, pH 4.0 citrate buffer solution and pH 6.8 phosphate buffer solution ($n = 3$, mean \pm SD).

intestinal survivability of active components in some extent and facilitate them to be successfully absorbed.

3.4. Enhanced hypoglycemic effect and bioavailability

In order to establish the optimal dose compatibility of mulberry leaf extracts/*Pueraria Lobata* extracts (M/P), we employed

different dosage ratios of extracts to fabricate MPE-SeNPs and investigated the hypoglycemic effect of various formulations in normal rats. The blood glucose curves of SD rats after oral administration of different formulations are presented in [Supporting Information Fig. S1](#). It was found that MPE-SeNPs with an M/P of 1:2 produced the best hypoglycemic effect. The dosage ratio was, hence, designated to prepare the follow-up MPE-SeNPs.

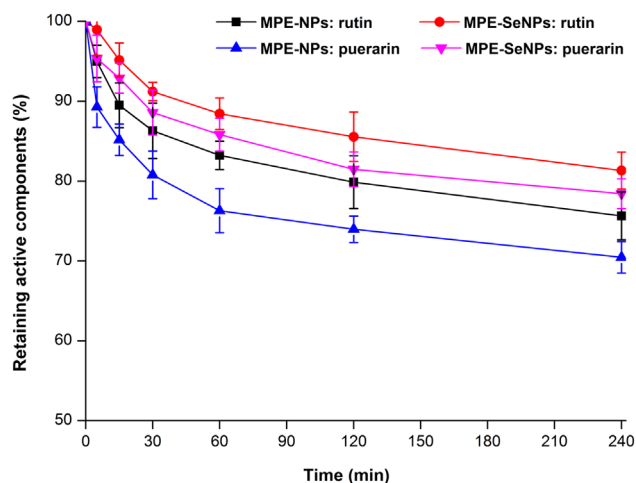


Figure 4 *In vitro* survivability of marker components (rutin and puerarin) in MPE-NPs or MPE-SeNPs studied in the simulated intestinal fluid containing intestinal microsomes ($n = 3$, mean \pm SD).

To further verify the hypoglycemic effect of MPE-SeNPs, diabetic rats were adopted for the blood glucose lowering test. Fig. 5 shows the blood glucose level change as a function of time in GK rats after treatment with different formulations. As shown in Fig. 5, the blood glucose of GK rats declined a little in the case of saline group. Of note, the blood glucose of GK rats in all oral administration groups went up within the first hours. The phenomenon of initial blood glucose surge due to force-feeding also appeared in previous reports^{36,46}. Blank SeNPs also gave rise to a certain hypoglycemic effect in comparison with saline, which may be connected with the insulin-mimetic effect of Se^{34,47}. MPE solution posed a relatively weak hypoglycemic effect. It stands to reason that MPE solution should exhibit a better pharmacological activity than any formulation, since in which the active components are molecularly existent. We suppose that it may be related to the poor absorption or intestinal metabolism of MPE. As reflected in MPE-NPs, the hypoglycemic effect of MPE was improved when loaded in nanoparticles. Compared with MPE-NPs, a more significant hypoglycemic effect took place in MPE-SeNPs, resulting in

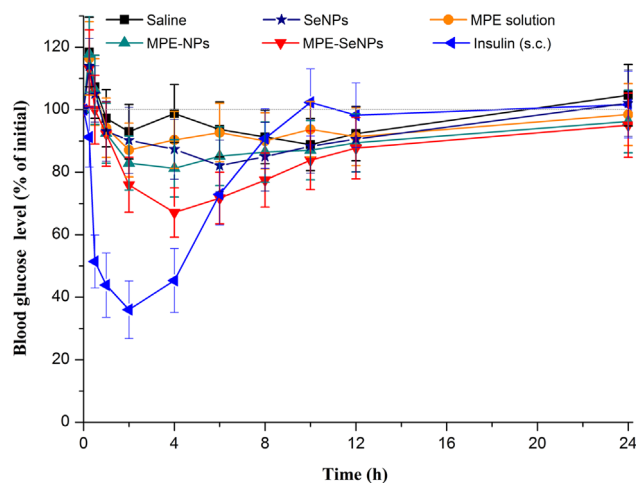


Figure 5 Blood glucose level vs. time curves in diabetic rats following oral administration of saline, SeNPs, MPE solution, MPE-NPs and MPE-SeNPs (equivalent to 125 μ g/kg MPE) and subcutaneous (s.c.) injection of insulin (1 IU/kg) ($n = 6$, mean \pm SD).

a maximal decline of blood glucose to 32.88%. At the dose of 125 mg/kg, MPE-SeNPs have caused a remarkable and sustained hypoglycemic effect in diabetic rats. MPE-SeNPs involve no any chemical antidiabetic agents, but they produce an appreciable hypoglycemic effect. This indicates that MPE has the hypoglycemic activity and there is a synergistic effect between MPE and SeNPs. The antidiabetic efficacies of MPE and SeNPs have been severally verified^{34,48-50}. Neither MPE nor SeNPs alone are able to produce satisfactory curative effects due to insufficient bioactivity and pathological complexity of DM. MPE-SeNPs complement each other's advantages and can cooperatively intervene DM through multiple pathways and targets. In addition, MPE-SeNPs not only can promote the oral absorption of MPE, but also can transport them to the liver, a vital organ responsible for glycometabolism, through the portal vein. The synergistic effect between MPE and SeNPs is reflected both in pharmacology and drug delivery.

The absorption-promoting effect of SeNPs on MPE can also be inferred from the pharmacokinetics of rutin and puerarin (Fig. 6).

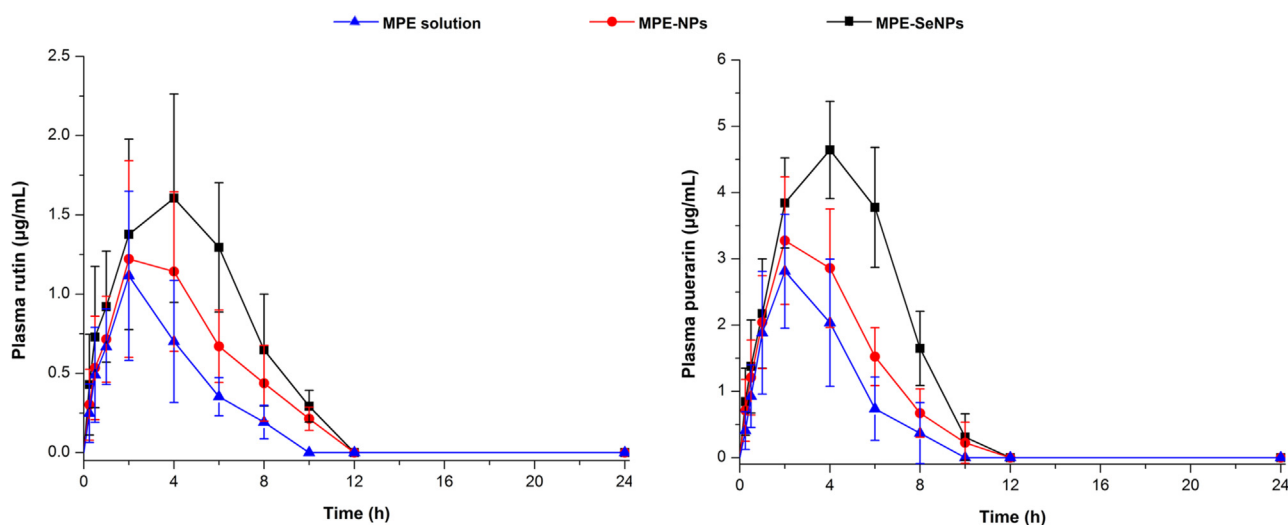


Figure 6 Plasma rutin and puerarin concentration vs time curves in diabetic rats after administration of MPE solution, MPE-NPs and MPE-SeNPs ($n = 6$, mean \pm SD).

Table 1 Main pharmacokinetic parameters of rutin and puerarin after oral administration of MPE solution, MPE-NPs and MPE-SeNPs ($n = 6$).

Compd.	Formulation	MPE solution	MPE-NPs	MPE-SeNPs
Rutin	C_{\max} ($\mu\text{g/mL}$)	1.12 ± 0.13	1.22 ± 0.18	$1.61 \pm 0.21^{**}$
Puerarin		2.81 ± 0.56	3.27 ± 0.45	$4.64 \pm 0.31^{**}$
Rutin	T_{\max} (h)	2.00 ± 0.37	2.00 ± 0.26	$4.00 \pm 0.36^{**}$
Puerarin		2.00 ± 0.23	2.00 ± 0.35	$4.00 \pm 0.42^{**}$
Rutin	AUC_{0-t}	4.72 ± 2.04	$7.36 \pm 3.31^{\ddagger}$	$10.53 \pm 2.46^{**}$
Puerarin	($\mu\text{g/mL} \cdot \text{h}$)	11.99 ± 2.27	$17.41 \pm 3.14^{\ddagger}$	$28.56 \pm 5.91^{**}$
Rutin	Relative BA (%)	/	155.9 ± 16.54	$223.1 \pm 10.02^{**}$
Puerarin		/	145.2 ± 13.25	$238.5 \pm 24.66^{**}$

BA: bioavailability calculated based on AUC_{0-t} ; ANOVA, $^{\dagger}P < 0.05$, $^{\ddagger}P < 0.01$, compared with MPE solution; $^{**}P < 0.01$, compared with MPE-NPs. /, not applicable.

Enhanced plasma rutin and puerarin levels were achieved by MPE-SeNPs. MPE-SeNPs resulted in a larger AUC (area under the curve of blood drug concentration vs. time) than MPE solution and MPE-NPs. The absorption characteristics among them were also significantly different. The time to maximum plasma concentration (T_{\max}) of MPE-SeNPs lagged behind MPE solution and MPE-NPs in terms of two marker components. It is indicative that SeNPs not only can promote MPE absorption, but also sustain them release. The main pharmacokinetic parameters of rutin and puerarin are listed in Table 1. The relative oral bioavailability of MPE-SeNPs to

MPE solution was up to 223.1% and 238.5% quantified by rutin and puerarin, respectively. Although the relative oral bioavailability of MPE was enhanced to 150% around by MPE-NPs, the ameliorative effect in oral bioavailability of MPE-NPs was significantly inferior to MPE-SeNPs. In this study, we used two quantitative substances to calculate the oral availability of MPE-SeNPs. The results bring out a striking similarity, proving the suitability of quantitative method. The enhanced hypoglycemic effect of MPE-SeNPs can be rationalized by increased absorption of MPE and the synergic effect of SeNPs in blood glucose homeostasis.

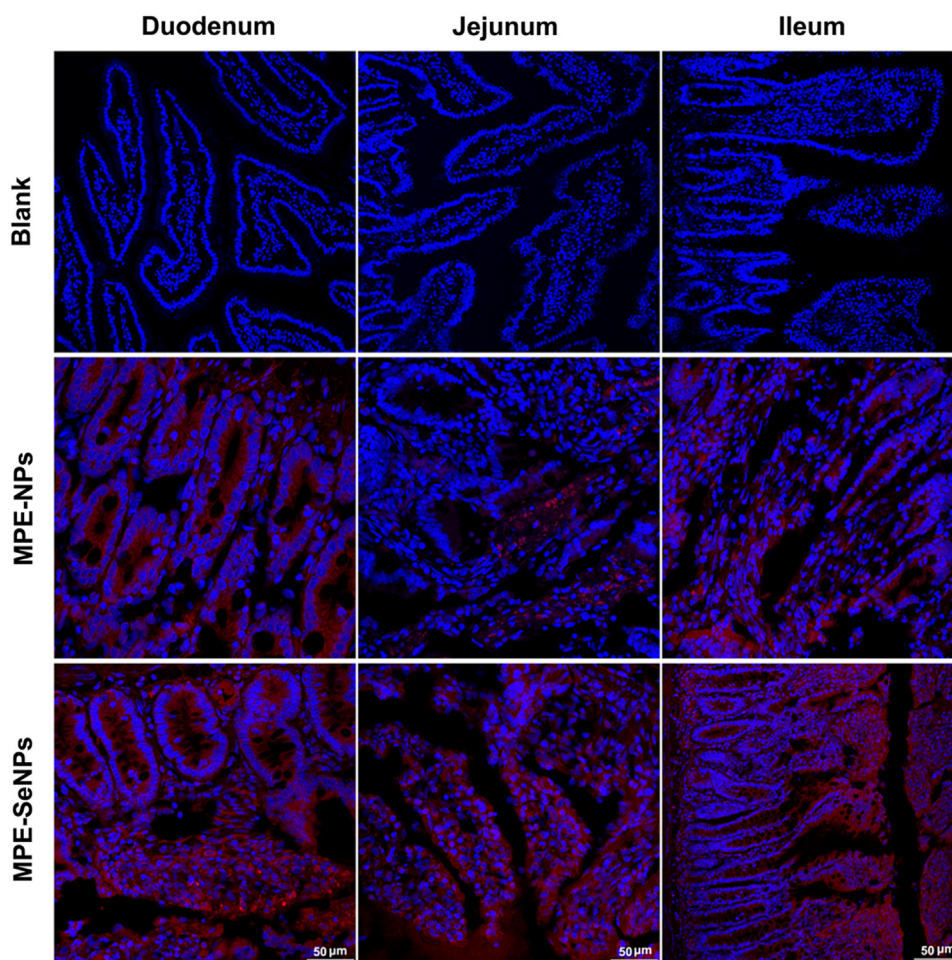


Figure 7 Ex vivo imaging of transepithelial transport of MPE-NPs and MPE-SeNPs inspected by CLSM. The absorptive epithelia were excised immediately from the diabetic rats at 2 h after oral administration of DiI-labeled MPE-NPs and MPE-SeNPs.

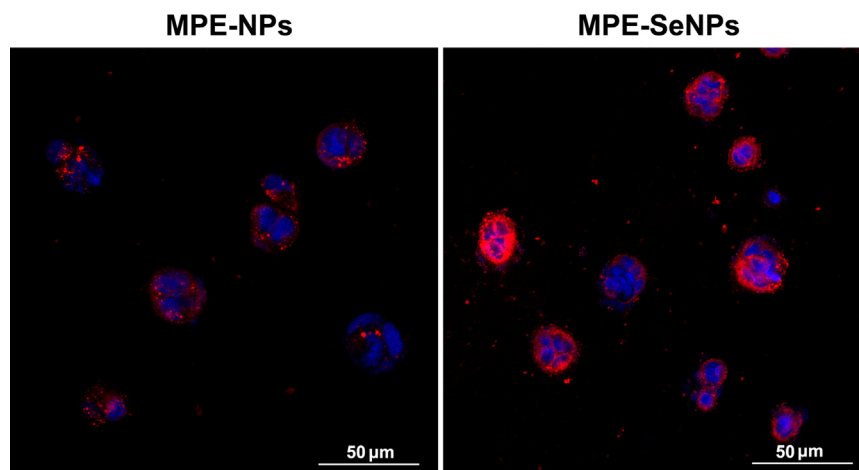


Figure 8 Cellular uptake of MPE-NPs and MPE-SeNPs characterized by confocal imaging: MPE-NPs and MPE-SeNPs in red with DiI and cell nuclei in blue with DAPI.

3.5. Oral absorption mechanisms

To appreciate the transepithelial transport of MPE-SeNPs, we investigated the intestinal permeability of nanoparticles by *ex vivo* imaging. Fig. 7 shows the epithelial staining of two kinds of nanoparticles in various intestinal segments 2 h after administration. We could clearly observe the intestinal villi from the longitudinal cross-section of tissue slices in the blank group. MPE-NPs only exhibited a weak fluorescence distribution in the absorptive epithelia. However, MPE-SeNPs resulted in an intense fluorescent infiltration that interspersed the whole intestinal epithelia. It indicates that MPE-SeNPs possess stronger intestinal affinity and permeability. The underlying causes may be associated with the high density of SeNPs and the oxidative stress of diabetic subjects. High density renders SeNPs easy to attach to the enterocytes. Diabetics generally have an aggravated oxidative stress that would like to assimilate more antioxidants to rescue the unbalanced system^{51,52}.

The cellular uptake of MPE-SeNPs was visually characterized by CLSM in comparison with MPE-NPs (Fig. 8). MPE-SeNPs showed more intense cellular internalization relative to MPE-NPs. This suggests considerable MPE-SeNPs have internalized into Caco-2 cells, even into the nuclei as shown by the localization. The cells treated with MPE-NPs merely exhibited a feeble fluorescent staining. These results accorded well with the *ex vivo* imaging of transepithelial transport. It also indicates that MPE-NPs and MPE-SeNPs share a different cellular trafficking pathway.

The cellular trafficking pathway of nanoparticles can be interpreted by the relative cellular uptake in the presence of special transport inhibitors⁵³. The relative cellular uptake of MPE-NPs and MPE-SeNPs under the action of inhibitors, quantified by rutin in MPE, is shown in Fig. 9. In the group of MPE-NPs, the cellular uptake was markedly inhibited by hypertonic sucrose and latrunculin B. Different from MPE-NPs, the cellular uptake of MPE-SeNPs was collectively inhibited by hypertonic sucrose, chlorpromazine, simvastatin and filipin. As known, latrunculin B is used as a macropinocytosis inhibitor. Hypertonic sucrose and chlorpromazine act as non-specific and specific clathrin-mediated endocytosis inhibitors; and simvastatin and filipin serve as non-specific and specific caveolin-mediated endocytosis inhibitors,

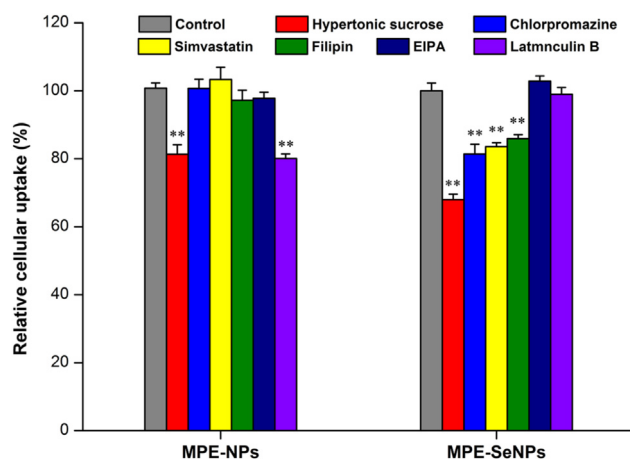


Figure 9 Relative cellular uptake of MPE-NPs and MPE-SeNPs in the presence of hypertonic sucrose (0.5 mol/L), chlorpromazine (25 μ mol/L), simvastatin (25 μ mol/L), filipin (1.0 μ mol/L), EIPA (50 μ mol/L) and latrunculin B (200 nmol/L). Paired *t*-test, $P < 0.01$, compared with the control.

respectively. From the experimental results, it can be concluded that nonspecific clathrin-mediated endocytosis and macropinocytosis are involved in the cellular transport of MPE-NPs, and clathrin- and caveolin-mediated endocytosis are the leading mechanisms responsible for the cellular transport of MPE-SeNPs. It has similarity and difference in the cellular trafficking pathway between MPE-NPs and MPE-SeNPs. Otherwise, MPE-SeNPs possess multiple endocytosis pathways, thus transporting into cells more easily. As known, pinocytosis is a transport mode of substances in which liquid droplets or small particles suspended in the extracellular fluid are brought into the cell through an invagination of the cell membrane; the transport objects of clathrin/caveolin-mediated endocytosis where forms coated vesicles in the cytomembrane are particles with a stronger rigidity⁵⁴. SeNPs possess a robust structure relative to conventional PLGA nanoparticles, which is why pinocytosis have not occurred on the cellular transport of MPE-SeNPs.

Table 2 Blood biochemical indices of GK rats after treatment with MPE-NPs or MPE-SeNPs for 14 days.

Group	MDA (nmol/mL)	ROS (IU/mL)	SOD (IU/mL)	GSH (mg/L)	GSH-Px (IU/mL)
Control	18.52 ± 1.28	895.26 ± 11.15	85.79 ± 1.22	305.26 ± 11.67	724.15 ± 21.35
MPE-NPs	15.27 ± 1.18*	868.25 ± 11.54	89.02 ± 1.42	338.25 ± 13.92*	781.24 ± 20.24*
MPE-SeNPs	12.87 ± 1.36**	851.67 ± 10.77*	91.24 ± 1.13*	364.18 ± 15.01**	813.15 ± 25.63**

Data are shown as the mean ± SD ($n = 3$). Statistical significance is done by paired t -test, * $P < 0.05$, ** $P < 0.01$, compared with the control.

From the above, the oral absorption mechanisms of MPE-SeNPs are related to superior intestinal permeability, fine cellular uptake and progressive cytolysis that facilitate MPE-SeNPs readily across the absorptive epithelia, thereby increasing the overall absorption of payload. MPE-SeNPs fluorescently overlay both with the cytoplasm and the nuclei. Nanoparticles can be taken up by cells through a certain kind of cytolysis (*e.g.*, clathrin-mediated endocytosis). To approach the nucleus, they have to escape from the vesicles (endosomes/lysosomes) they are trapped in. After release in the cytoplasm, they can connect to the nuclear pore and complex with some peptide sequence (nuclear localization signal, NLS) and then enter the nuclei⁵⁵. It seems simple, though this does not tend to take place, which depends on the size and charge matters of nanoparticles. MPE-SeNPs entering the nuclei may be associated with some specific NLS to positive charged MPE-SeNPs. Although the anti-oxidant effect of MPE mainly occurs in the cytoplasm, fractional nuclear uptake of MPE-SeNPs would not compromise the antioxidant effect of MPE, since MPE can be released from nuclei when SeNPs are degraded by oxidation.

3.6. Anti-diabetic mechanisms

The oxidative stress in patients can be estimated by the levels of ROS, MDA, SOD and GSH as well as the activity of GSH-Px. Table 2 gives the biochemical values of GK rats on ROS, MDA, SOD, GSH and GSH-Px after treatment with MPE-NPs or MPE-SeNPs for two weeks. MPE-NPs just resulted in a slight decline of MDA and mild increases of GSH and GSH-Px in diabetic rats. We

assume that it is associated with the weak antioxidation activity of MPE. The antioxidative potency of MPE is relatively inadequate that thus difficultly produces a significant antioxidative effect. Of note, MPE-SeNPs caused significant decline of all peroxides (MDA and ROS) and increase of all antioxidants (SOD, GSH and GSH-Px), demonstrating more potent antioxidation capacity than MPE-NPs. It can be attributed to the participation of Se. For one thing, Se constitutes the active center of GSH-Px and provides selenol to GSH to exert the antioxidative activity⁵⁶; for another, Se can reduce the levels of peroxides by spontaneous oxidation *in vivo*. Diabetics show elevated level of peroxides and decreased activity of antioxidant enzymes. Our developed MPE-SeNPs can alleviate the oxidative stress of diabetic subjects by regulating the peroxide and antioxidant levels, which is fairly beneficial for diabetic care.

Pancreatic β cells are the prime targets of attack from oxidative stress and inflammation as a result of hyperglycemia. Pancreatic β cells have an extremely limited regenerative potential, especially for type 1 DM. Fig. 10 shows the immunohistochemical outcomes of pancreatic islet of GK rats before and after treatment with MPE-NPs or MPE-SeNPs. There was only a small amount of living β cells observable in the pancreatic islet of diabetic rats before treatment. After treatment for two weeks, the amount of living β cells in the pancreatic islet significantly increased both in the case of MPE-NPs and MPE-SeNPs. The improvement in β cell activity was more conspicuous in the group of MPE-SeNPs, showing a dramatic restoration of impaired β -cells. It should bear in mind that lowering the blood glucose of diabetic patients is not the ultimate goal that is to repair the impaired pancreatic islet.

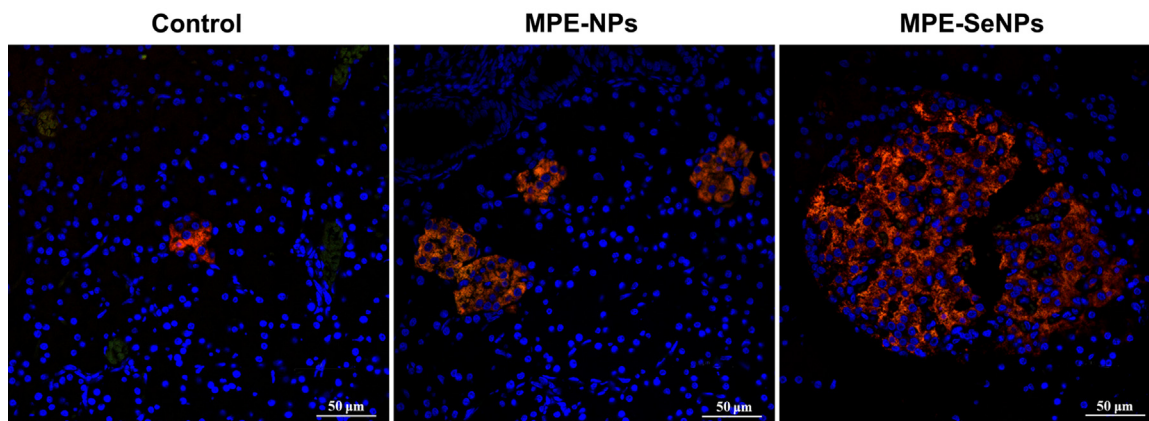


Figure 10 Fluorescent histomorphologies of pancreatic islet of diabetic rats before and after treatment with MPE-NPs or MPE-SeNPs for two weeks. The pancreatic islet are specifically labeled by Cy3-conjugated antibody to insulin (red) and DAPI (blue). After treatment, the insulin-secreting cells sharply increased.

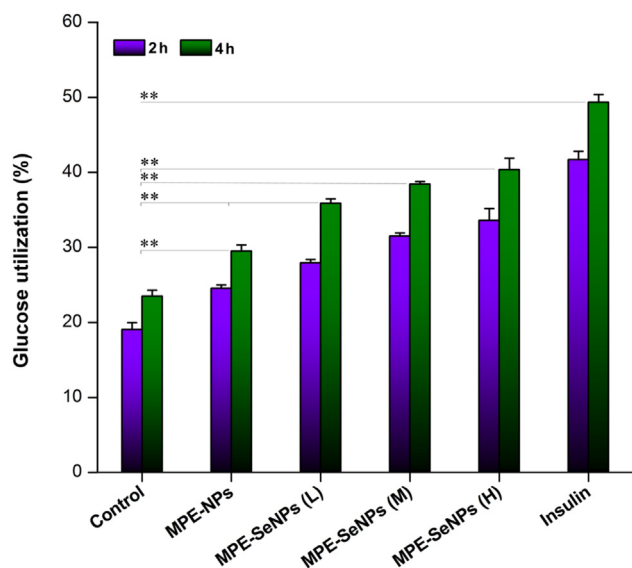


Figure 11 Glucose utilization in the adipocytes in the presence of MPE-NPs (1.0 $\mu\text{g}/\text{mL}$) or MPE-SeNPs (L: 1.0 $\mu\text{g}/\text{mL}$; M: 1.5 $\mu\text{g}/\text{mL}$; H: 2.0 $\mu\text{g}/\text{mL}$), blank culture medium as negative control and insulin (1.0 $\mu\text{g}/\text{mL}$, ~ 0.025 IU/mL) as positive control, respectively. Independent sample *t*-test, **P* < 0.01, significantly different between two groups.

To further verify the hypoglycemic activity of MPE-SeNPs, we successfully constructed adipocytes from ADSCs using IBMX. ADSCs transformed from fusiform without fat bubble to a circle or ellipse shape with large fat bubbles observable, implying the formation of adipocytes (Supporting Information Fig. S2). The glucose utilization in adipocytes notably increased in the presence of MPE-NPs and MPE-SeNPs compared to the control (Fig. 11). Both MPE-NPs and MPE-SeNPs could facilitate adipocytes to assimilate glucose. MPE-SeNPs exhibited a stronger promoting effect on glucose utilization than MPE-NPs as for the extent. In addition, it showed a dose- and time-dependent trend in the glucose utilization. Of note, the potency of MPE-SeNPs (2.0 $\mu\text{g}/\text{mL}$) was close to that of 1.0 $\mu\text{g}/\text{mL}$ of insulin (0.025 IU/mL), which was rather amazing in glucose biotransformation in terms of natural medications. The results demonstrate that MPE-SeNPs possess an insulin-mimetic effect and can synergistically cure DM by way of reducing oxidative stress, improving pancreatic function and promoting glucose utilization.

4. Conclusions

This work conducts a careful insight into the combination of the traditional Chinese medicine and Se supplement for DM treatment. MPE-SeNPs showed a high encapsulation for MPE and could stabilize the payload in the harsh GI conditions. MPE-SeNPs produced a remarkable and long-acting hypoglycemic effect following oral administration to diabetic rats. The oral bioavailability of MPE was significantly enhanced through SeNPs depending on the excellent intestinal permeability and transepithelial transport. In addition to the insulin-mimetic action, MPE-SeNPs demonstrated multiple antidiabetic effects that could alleviate the oxidative stress *in vivo*, improve the

pancreatic function and accelerate the glucose utilization by adipocytes. These findings provide a proof of concept that phytomedicine and selenium can be effectively integrated into nanomedicine to fight against DM, over and above the case of MPE-SeNPs.

Acknowledgements

This work was financially supported by the National Natural Science Foundation of China (81673604) and the Fundamental Research Funds for the Central Universities (21617473, China).

Appendix A. Supporting information

Supplementary data associated with this article can be found in the online version at <https://doi.org/10.1016/j.apsb.2018.09.009>.

References

1. Elwood WN, Huss K, Morales DA, Norton JM, Riddle MW, Roof RA, et al. NIH research opportunities for the prevention and treatment for chronic conditions. *Transl Behav Med* 2018;**8**:509–14.
2. Fonseca VA. New developments in diabetes management: medications of the 21st century. *Clin Ther* 2014;**36**:477–84.
3. Li WL, Zheng HC, Bukuru J, De Kimpe N. Natural medicines used in the traditional Chinese medical system for therapy of diabetes mellitus. *J Ethnopharmacol* 2004;**92**:1–21.
4. Wang E, Wylie-Rosett J. Review of selected Chinese herbal medicines in the treatment of type 2 diabetes. *Diabetes Educ* 2008;**34**:645–54.
5. Lu Y, Li Y, Wu W. Injected nanocrystals for targeted drug delivery. *Acta Pharm Sin B* 2016;**6**:106–13.
6. He H, Lu Y, Qi J, Zhu Q, Chen Z, Wu W. Adapting liposomes for oral drug delivery. *Acta Pharm Sin B* 2018. Available from: <http://dx.doi.org/10.1016/j.apsb.2018.06.005>.
7. Li F, Hu R, Wang B, Gui Y, Cheng G, Gao S, et al. Self-microemulsifying drug delivery system for improving the bioavailability of huperzine A by lymphatic uptake. *Acta Pharm Sin B* 2017;**7**:353–60.
8. Jin K, Luo Z, Zhang B, Pang Z. Biomimetic nanoparticles for inflammation targeting. *Acta Pharm Sin B* 2018;**8**:23–33.
9. Cui M, Wu W, Hovgaard L, Lu Y, Chen D, Qi J. Liposomes containing cholesterol analogues of botanical origin as drug delivery systems to enhance the oral absorption of insulin. *Int J Pharm* 2015;**489**:277–84.
10. Zhang X, Qi J, Lu Y, He W, Li X, Wu W. Biotinylated liposomes as potential carriers for the oral delivery of insulin. *Nanomedicine* 2014;**10**:167–76.
11. He H, Lu Y, Qi J, Zhao W, Dong X, Wu W. Biomimetic thiamine- and niacin-decorated liposomes for enhanced oral delivery of insulin. *Acta Pharm Sin B* 2018;**8**:97–105.
12. Kassem AA, Abd El-Alim SH, Basha M, Salama A. Phospholipid complex enriched micelles: a novel drug delivery approach for promoting the antidiabetic effect of repaglinide. *Eur J Pharm Sci* 2017;**99**:75–84.
13. Alai MS, Lin WJ, Pingale SS. Application of polymeric nanoparticles and micelles in insulin oral delivery. *J Food Drug Anal* 2015;**23**:351–8.
14. Li X, Qi J, Xie Y, Zhang X, Hu S, Xu Y, et al. Nanoemulsions coated with alginate/chitosan as oral insulin delivery systems: preparation, characterization, and hypoglycemic effect in rats. *Int J Nanomed* 2013;**8**:23–32.
15. Goncalves LM, Maestrelli F, Di Cesare Mannelli L, Ghelardini C, Almeida AJ, Mura P. Development of solid lipid nanoparticles as

- carriers for improving oral bioavailability of glibenclamide. *Eur J Pharm Biopharm* 2016;**102**:41–50.
16. Ansari MJ, Anwer MK, Jamil S, Al-Shdefat R, Ali BE, Ahmad MM, et al. Enhanced oral bioavailability of insulin-loaded solid lipid nanoparticles: pharmacokinetic bioavailability of insulin-loaded solid lipid nanoparticles in diabetic rats. *Drug Deliv* 2016;**23**:1972–9.
 17. Sheng J, Han L, Qin J, Ru G, Li R, Wu L, et al. *N*-Trimethyl chitosan chloride-coated PLGA nanoparticles overcoming multiple barriers to oral insulin absorption. *ACS Appl Mater Interfaces* 2015;**7**:15430–41.
 18. Liu C, Shan W, Liu M, Zhu X, Xu J, Xu Y, et al. A novel ligand conjugated nanoparticles for oral insulin delivery. *Drug Deliv* 2016;**23**:2015–25.
 19. Shan W, Zhu X, Liu M, Li L, Zhong J, Sun W, et al. Overcoming the diffusion barrier of mucus and absorption barrier of epithelium by self-assembled nanoparticles for oral delivery of insulin. *ACS Nano* 2015;**9**:2345–56.
 20. Wong CY, Al-Salami H, Dass CR. Potential of insulin nanoparticle formulations for oral delivery and diabetes treatment. *J Control Release* 2017;**264**:247–75.
 21. Wagner AM, Gran MP, Peppas NA. Designing the new generation of intelligent biocompatible carriers for protein and peptide delivery. *Acta Pharm Sin B* 2018;**8**:147–64.
 22. Wang X, Liu Q, Zhu H, Wang H, Kang J, Shen Z, et al. Flavanols from the *Camellia sinensis* var. *assamica* and their hypoglycemic and hypolipidemic activities. *Acta Pharm Sin B* 2017;**7**:342–6.
 23. Pang B, Zhao LH, Zhou Q, Zhao TY, Wang H, Gu CJ, et al. Application of berberine on treating type 2 diabetes mellitus. *Int J Endocrinol* 2015:905749.
 24. Li JB, Zhang R, Han X, Piao CL. Ginsenoside Rg1 inhibits dietary-induced obesity and improves obesity-related glucose metabolic disorders. *Braz J Med Biol Res* 2018;**51**:e7139.
 25. Chen X, Wang L, Fan S, Song S, Min H, Wu Y, et al. Puerarin acts on the skeletal muscle to improve insulin sensitivity in diabetic rats involving mu-opioid receptor. *Eur J Pharmacol* 2018;**818**:115–23.
 26. Xue M, Yang MX, Zhang W, Li XM, Gao DH, Ou ZM, et al. Characterization, pharmacokinetics, and hypoglycemic effect of berberine loaded solid lipid nanoparticles. *Int J Nanomed* 2013;**8**:4677–87.
 27. Yin J, Hou Y, Yin Y, Song X. Selenium-coated nanostructured lipid carriers used for oral delivery of berberine to accomplish a synergic hypoglycemic effect. *Int J Nanomed* 2017;**12**:8671–80.
 28. Ge Q, Chen L, Tang M, Zhang S, Gao L, Ma S, et al. Analysis of mulberry leaf components in the treatment of diabetes using network pharmacology. *Eur J Pharmacol* 2018;**833**:50–62.
 29. Sheng Y, Zheng S, Ma T, Zhang C, Ou X, He X, et al. Mulberry leaf alleviates streptozotocin-induced diabetic rats by attenuating NEFA signaling and modulating intestinal microflora. *Sci Rep* 2017;**7**:12041.
 30. Tanaka T, Yokota Y, Tang H, Zaima N, Moriyama T, Kawamura Y. Anti-hyperglycemic effect of a Kudzu (*Pueraria lobata*) Vine extract in ovariectomized mice. *J Nutr Sci Vitaminol* 2016;**62**:341–9.
 31. Seong SH, Roy A, Jung HA, Jung HJ, Choi JS. Protein tyrosine phosphatase 1B and α -glucosidase inhibitory activities of *Pueraria lobata* root and its constituents. *J Ethnopharmacol* 2016;**194**:706–16.
 32. Ozturk Z, Gurpinar T, Vural K, Boyacioglu S, Korkmaz M, Var A. Effects of selenium on endothelial dysfunction and metabolic profile in low dose streptozotocin induced diabetic rats fed a high fat diet. *Biotech Histochem* 2015;**90**:506–15.
 33. Bahmani F, Kia M, Soleimani A, Mohammadi AA, Asemi Z. The effects of selenium supplementation on biomarkers of inflammation and oxidative stress in patients with diabetic nephropathy: a randomised, double-blind, placebo-controlled trial. *Br J Nutr* 2016;**116**:1222–8.
 34. Al-Quraishy S, Dkhil MA, Abdel Moneim AE. Anti-hyperglycemic activity of selenium nanoparticles in streptozotocin-induced diabetic rats. *Int J Nanomed* 2015;**10**:6741–56.
 35. Peng CH, Lin HT, Chung DJ, Huang CN, Wang CJ. Mulberry leaf extracts prevent obesity-induced NAFLD with regulating adipocytokines, inflammation and oxidative stress. *J Food Drug Anal* 2018;**26**:778–87.
 36. Deng W, Xie Q, Wang H, Ma Z, Wu B, Zhang X. Selenium nanoparticles as versatile carriers for oral delivery of insulin: insight into the synergic antidiabetic effect and mechanism. *Nanomedicine* 2017;**13**:1965–74.
 37. Yin J, Wang P, Yin Y, Hou Y, Song X. Optimization on biodistribution and antitumor activity of tripteryne using polymeric nanoparticles through RES saturation. *Drug Deliv* 2017;**24**:1891–7.
 38. Hu S, Niu M, Hu F, Lu Y, Qi J, Yin Z, et al. Integrity and stability of oral liposomes containing bile salts studied in simulated and *ex vivo* gastrointestinal media. *Int J Pharm* 2013;**441**:693–700.
 39. Sun H, Liu H, Zhao H, Wang Y, Li YL, Ye WC, et al. Pharmacokinetic characterization of anhuienoside C and its deglycosylated metabolites in rats. *Xenobiotica* 2017;**47**:885–93.
 40. Zhang M, Xu C, Liu D, Han MK, Wang L, Merlin D. Oral delivery of nanoparticles loaded with ginger active compound, 6-shogaol, attenuates ulcerative colitis and promotes wound healing in a murine model of ulcerative colitis. *J Crohns Colitis* 2018;**12**:217–29.
 41. Jensen DK, Jensen LB, Koocheki S, Bengtson L, Cun D, Nielsen HM, et al. Design of an inhalable dry powder formulation of DOTAP-modified PLGA nanoparticles loaded with siRNA. *J Control Release* 2012;**157**:141–8.
 42. Xie Q, Deng W, Yuan X, Wang H, Ma Z, Wu B, et al. Selenium-functionalized liposomes for systemic delivery of doxorubicin with enhanced pharmacokinetics and anticancer effect. *Eur J Pharm Biopharm* 2018;**122**:87–95.
 43. Ray S, Ghosh Ray S, Mandal S. Development of bicalutamide-loaded PLGA nanoparticles: preparation, characterization and *in-vitro* evaluation for the treatment of prostate cancer. *Artif Cells Nanomed Biotechnol* 2017;**45**:944–54.
 44. Li YJ, Hu XB, Lu XL, Liao DH, Tang TT, Wu JY, et al. Nanoemulsion-based delivery system for enhanced oral bioavailability and Caco-2 cell monolayers permeability of berberine hydrochloride. *Drug Deliv* 2017;**24**:1868–73.
 45. Zhang J, Wang D, Wu Y, Li W, Hu Y, Zhao G, et al. Lipid-polymer hybrid nanoparticles for oral delivery of tartary buckwheat flavonoids. *J Agric Food Chem* 2018;**66**:4923–32.
 46. Niu M, Lu Y, Hovgaard L, Guan P, Tan Y, Lian R, et al. Hypoglycemic activity and oral bioavailability of insulin-loaded liposomes containing bile salts in rats: the effect of cholate type, particle size and administered dose. *Eur J Pharm Biopharm* 2012;**81**:265–72.
 47. Ueno H, Shimizu R, Okuno T, Ogino H, Arakawa T, Murano K, et al. Effect of seleno-L-methionine on oxidative stress in the pancreatic islets of a short-term induced diabetic mouse model in insufficient selenium status. *Biol Pharm Bull* 2018;**41**:80–5.
 48. Riche DM, Riche KD, East HE, Barrett EK, May WL. Impact of mulberry leaf extract on type 2 diabetes (Mul-DM): a randomized, placebo-controlled pilot study. *Complement Ther Med* 2017;**32**:105–8.
 49. Prasain JK, Peng N, Rajbhandari R, Wyss JM. The Chinese Pueraria root extract (*Pueraria lobata*) ameliorates impaired glucose and lipid metabolism in obese mice. *Phytomedicine* 2012;**20**:17–23.
 50. Liu Y, Zeng S, Liu Y, Wu W, Shen Y, Zhang L, et al. Synthesis and antidiabetic activity of selenium nanoparticles in the presence of polysaccharides from *Catathelasma ventricosum*. *Int J Biol Macromol* 2018;**114**:632–9.
 51. Keane KN, Cruzat VF, Carlessi R, de Bittencourt PI Jr, Newsholme P. Molecular events linking oxidative stress and inflammation to insulin resistance and β -cell dysfunction. *Oxid Med Cell Longev* 2015;**2015**:181643.

52. Gonzalez de Vega R, Fernandez-Sanchez ML, Fernandez JC, Alvarez Menendez FV, Sanz-Medel A. Selenium levels and glutathione peroxidase activity in the plasma of patients with type II diabetes mellitus. *J Trace Elem Med Biol* 2016;**37**:44–9.
53. Fan T, Chen C, Guo H, Xu J, Zhang J, Zhu X, et al. Design and evaluation of solid lipid nanoparticles modified with peptide ligand for oral delivery of protein drugs. *Eur J Pharm Biopharm* 2014;**88**:518–28.
54. Mukherjee S, Ghosh RN, Maxfield FR. Endocytosis. *Physiol Rev* 1997;**77**:759–803.
55. Misra R, Sahoo SK. Intracellular trafficking of nuclear localization signal conjugated nanoparticles for cancer therapy. *Eur J Pharm Sci* 2010;**39**:152–63.
56. Chomchan R, Puttarak P, Brantner A, Siripongvutikorn S. Selenium-rich ricegrass juice improves antioxidant properties and nitric oxide inhibition in macrophage cells. *Antioxidants (Basel)* 2018;**7**:E57.